JOURNAL OF Applied Polymer SCIENCE

Melt-Spun Polylactic Acid Fibers: Effect of Cellulose Nanowhiskers on Processing and Properties

Maya Jacob John,[1,2] Rajesh Anandjiwala,[1,2] Kristiina Oksman,[3,4] Aji P Mathew[3,4]

[1]CSIR, Materials Science and Manufacturing, Polymers and Composites, Port Elizabeth, South Africa
[2]Department of Textile Science, Nelson Mandela Metropolitan University, P.O. Box 1600, Port Elizabeth 6000, South Africa
[3]Division of Materials Science, Luleå University of Technology, 97187 Luleå, Sweden
[4]Composite Centre Sweden, Luleå University of Technology, 97187 Luleå, Sweden

Correspondence to: A. Mathew (E-mail: aji.mathew@ltu.se)

ABSTRACT: Bio-based continuous fibers were processed from polylactic acid (PLA) and cellulose nanowhiskers (CNWs) by melt spinning. Melt compounding of master batches of PLA with 10 wt % CNWs and pure PLA was carried out using a twin-screw extruder in which compounded pellets containing 1 and 3 wt % of CNWs were generated for subsequent melt spinning. The microscopy studies showed that the fiber diameters were in the range of 90-95 μm, and an increased surface roughness and aggregations in the fibers containing CNWs could be detected. The addition of the CNWs restricted the drawability of the fibers to a factor of 2 and did not affect the fiber stiffness or strength, but resulted in a significantly lower strain and slightly increased crystallinity. Furthermore, CNWs increased the thermal stability, creep resistance and reduction in thermal shrinkage of PLA fibers, possibly indicating a restriction of the polymer chain mobility due to the nanoscale additives. © 2012 Wiley Periodicals, Inc. J. Appl. Polym. Sci. 000: 000–000, 2012

KEYWORDS: melt spinning; polylactic acid; cellulose nanowhiskers; mechanical properties; thermal properties; shrinkage

Received 23 January 2012; accepted 12 April 2012; published online
DOI: 10.1002/app.37884

INTRODUCTION

In comparison to other methods, such as solution-spinning or electrospinning, which have low throughput rates and require solvents to dissolve the polymers,[1] melt spinning is one of the most economical and convenient methods for manufacturing continuous fibers from polymers. An important advantage of the melt spinning route is the large quantity of fine fibers that can be produced by extrusion and the possibility for fiber-drawing and heat setting to increase the dimensional stability.[2] Synthetic fibers were commercialized in the 1950s; polyethylene terephthalate (PET) fibers being the highest volume produced mainly for textile applications.[3] Fibers have also been produced from polyamides, polyesters, poly-acrylonitrile, polyolefins, polyurethane, polyvinyl alcohol, and extensively used in diverse applications like textiles, filters, protective clothing, reinforcement in tyres, and composites.[4] However, more recently, polylactic acid (PLA), a polyester obtained from renewable resources has been extensively explored for fiber applications due to its similarity with PET fibers, eco-friendly nature, chemical resistance, barrier properties, and ease of processing.[5] In the current scenario, PLA-based fibers seem to be one of the most promising candidates for future industrial applications, and there is a strong demand to expand and optimize potential applications by using various functional additives like reinforcements, plasticizers, or other polymers.

Recently, fiber technologies that enhance the physical properties and spinnability of polymers by the incorporation of additives have been developed.[6] However, most macro-sized reinforcements are not suitable for fiber spinning, as they can easily lead to spin-line failures because of the sizes, which are in the range of the fiber itself. On the other hand, nano-sized reinforcements are more likely to improve the fiber properties without affecting the spinnability and surface finish of the fibers.[7] The production of multifilament yarns based on polymer nanocomposites was first reported in 2002, where polyamide 6 (PA6) was used as matrix and Cloisite 30B was used as reinforcement.[8] Later on, nanocomposite-based fibers were developed using nylon -6,[9,10] PET,[11–13] polypropylene (PP)[7] polyamide-imide,[14] and PLA,[2,15–17] etc. Different types of nanoreinforcements like nanoclays, carbon nanotubes, and inorganic oxides have been used to reinforce PLA.[18] It is also expected that the drawing of the fibers during melt spinning leads to orientation of nanoreinforcements

Table I. Master Batch Formulations for Compound Used for Fiber Processing

	Master batch (g)				
Materials	PLA	CNW	Acetone/Chloroform	Bulk PLA (g)	Final composition (%)
PLA	20	0	60/140[a]	180	100
PLA-CNW$_1$	18	2	60/140[a]	180	99/1
PLA-CNW$_3$	54	6	120/420[a]	140	97/3

[a] *Solvent mixture removed during masterbatch preparation*

in the fibers, which might result in high-performance nanocomposite fibers. Literature survey reveals that clay reinforced PLA fibers were successfully developed by Solarski et al.[15] for textile applications. However, there was no improvement in mechanical properties after the addition of nanoclay. In another study, Potschke et al.[16] developed multiwalled carbon nanotube reinforced PLA fibers with promising results for sensor applications. The reports so far suggest that this is a promising route to produce continuous fibers for various applications and further research and process optimizations are required in this area.

During the melt spinning of a bio-based matrix like PLA, it is desirable to have bio-based reinforcements to retain the renewable nature of the fibers. PLA fibers with bio-based nanoadditive as cellulose nanowhiskers (CNWs) have not been reported to date. CNWs have emerged as one of the most interesting bio-based nano-reinforcements in the last decade. CNWs are available as an aqueous suspension of highly crystalline, nanoscaled, whisker-shaped rods, the dimensions of which are dependent on the cellulose origin and the hydrolysis conditions, such as time, temperature, and purity of materials.[19] Wood-based CNWs are about 3–10 nm in diameter and 100–300 nm in length.[20] The high aspect ratio, specific properties and surface area of CNWs contribute to superior mechanical properties making them a favorable nano-reinforcement in polymers. The use of CNWs in PLA has been well documented and several studies have been reported by Oksman and coworkers on this topic.[21,22] However, fiber spinning of PLA with nanowhiskers has been reported to a very limited extent, except for a recent study in which PLA fibers containing nanowhiksers were prepared by electrospinning.[23]

In this article, the attempt was to prepare continuous bio-fibers, with and without cellulosic nanoadditive, by the melt spinning process. Through the judicious selection of the cellulose nanowhisker content and processing conditions, the resulting fibers can be engineered to have enhanced properties. The main focus in this study is on the processing conditions and mechanical properties of the nanocomposite fibers. Analytical techniques like microscopy, mechanical testing and thermal analysis were used to characterize the melt-spun fibers.

EXPERIMENTAL

Materials

PLA: ESUN™ (melt spinning grade) purchased from Shenzhen Bright China Industrial Company, China was used as the matrix phase. The used PLA has a density of 1.24 g/cm^3 and t a melt flow index of 20 g/10 min at 190°C/2.16 kg, as reported by the material supplier. The CNWs, used as the reinforcing phase, were isolated from microcrystalline cellulose by sulphuric acid hydrolysis following the procedure reported by Bondeson et al.[24] Chloroform and acetone were purchased from Merck (Darmstadt, Germany) and used in preparation of the master batch.

Processing of Nanocomposites. Nanocomposite fibers were prepared using a three-step process. The initial step was the preparation of master batch using a solvent mixture followed by the extrusion step to form the pellets. The third step was melt spinning the pellets in a filament extruder to produce the nanocomposite fibers.

Preparation of the Master Batch. An adequate amount of PLA (refer to Table I) for each sample was weighed and completely dissolved in a solvent mixture of acetone and chloroform in the ratio of 9:1 by stirring at 55°C. The nanofibers in aqueous medium were solvent-exchanged to acetone by a series of centrifuging and redispersing steps. After that, different mixtures of PLA and nanofibers were prepared by mixing the acetone-based nanofiber suspensions with dissolved PLA (see Table I). Then, the mixture was cast in Petri dishes and allowed to evaporate overnight at room temperature followed by oven vacuum drying at 55°C for 8 h. The composite films obtained from the casting were crushed using a kitchen blender until a particulate material was obtained.

Compounding Extrusion. Nanocomposite pellets were manufactured using a twin-screw extruder, Coperion W&P ZSK 18 MEGALab (Stuttgart, Germany), with a screw speed of 120 rpm. The temperature profile was varied from 165°C at the feeding zone to 200°C at the die. The crushed master batch was dry-mixed with PLA, diluting it to 1 and 3 wt % cellulose whisker contents. The mixtures were vacuum-dried at 55°C for 8 h before the process whereby the PLA and its nanocomposites were compounded, followed by the pelletizing step. The formulations of prepared materials are presented in Table I.

Melt Spinning. Multifilament yarns were produced from the extruded pellets in a laboratory-scale extruder. The apparatus has a small extruder, a die for multifilament production, a first set of uptake godets, a set of heated godets (at the same velocity as the uptake godets), a fast godet, a relaxation godet and a winder. The temperature profile was varied from 190°C at the feeding zone to 210°C at the die. After extrusion, the filaments were cooled by air with a fan. The uptake velocity varied between 2 and 15 m/min, and the maximum winding speed was about 100 m/min. In all cases, the draw ratio was kept

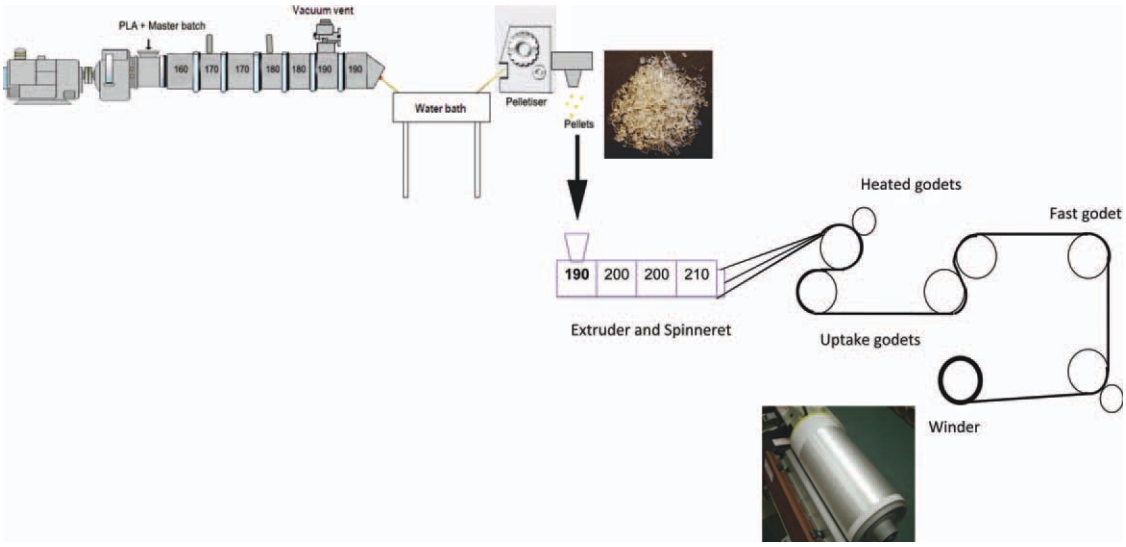

Figure 1. Schematic representation of the compounding followed by melt spinning of PLA and PLA–CNW fibers. [Color figure can be viewed in the online issue, which is available at wileyonlinelibrary.com.]

constant at 2. A schematic representation of the process is given in Figure 1.

Characterization

Scanning Electron Microscopy. A JEOL JSM-6460LV scanning electron microscope (SEM) was used to investigate the morphology of the fibers and to determinate their diameters. The fibers were previously sputter-coated with a gold layer of 40 nm to avoid charging. The acceleration voltage used was 5 kV.

Atomic Force Microscopy. The dispersion of cellulose whiskers in the melt-spun nanocomposite fibers was observed using an atomic force microscope (Veeco, Multimode, Nanoscope V) operated in tapping mode using RTESPW tip at a scanning rate of 0.498 Hz. Height and phase images were captured.

Mechanical Properties. DMA Q800 TA Instruments in tensile mode was used to study the tensile properties. In all cases, the tests were conducted on single fibers, with a gauge length of 15 mm at a constant rate of displacement of 1mm/min, under a constant temperature of 25°C. Four samples were tested for each material and the results are presented as an average of these.

Creep tests were performed using the DMA under creep mode. A static load of 5 MPa was applied on the fibers of 15-mm length. The test was performed in air atmosphere at room temperature for 10 min. The creep recovery was recorded by unloading samples for an additional 10 min. Three samples were tested for each material and the data presented are based on the agreeing measurements.

Thermal Analysis. Differential scanning calorimetry (DSC) was performed on Perkin Elmer Diamond DSC at 10°C/min from 30 to 200°C. The thermal properties, such as glass transition temperature (T_g), cold crystallization temperature (T_{cc}), melt temperature (T_m), and enthalpy of melting (ΔH_m) were determined from the heating scan of the samples. The crystallinity (%) of PLA was estimated from the corrected enthalpy for biopolymer content in the PLA nanocomposites, using the ratio between the heat of fusion of the studied polymer and the heat of fusion of the totally crystalline polymer, i.e.,

$$X_c = \frac{\Delta H_f}{\Delta H_f^0} \quad (1)$$

where, ΔH_f is the enthalpy of fusion of the studied specimen and ΔH_f^0 is the enthalpy of fusion of a totally crystalline material. The ΔH_f^o used in equation 1 was 93 J/g for PLA.[25,26]

Thermogravimetric analysis (TGA) was performed on a Perkin Elmer Pyris. The scanning rate was at 10°C/min and the temperature range was from 30 to 600°C in N_2 atmosphere.

The thermal shrinkage of PLA fibers, with and without the nanowhiskers, was measured at 80°C. The fibers (with initial length L_0) were heated in a hot air oven for 10 min without any tension. The fibers were then kept at room conditions for 20 min and the length (L_1) was measured. Thermal shrinkage was calculated according to the equation:

$$\text{Thermalshrinkage}(\%) = \frac{(L_0 - L_1) \times 100}{L_0} \quad (2)$$

RESULTS AND DISCUSSION

Processing of PLA fibers With and Without Nanoadditive

Nanocomposite fibers were prepared using a three-step process involving (1) Master batch preparation, (2) extrusion compounding, and (3) melt spinning. The initial step is the preparation of master batch using acetone/chloroform solvent mixture. It was expected that mixing of CNWs with PLA in a solvent medium would facilitate the dispersion. In the compounding step using the twin-screw extruder, the master batch was diluted with PLA pellets and distributed throughout the final compound. This step allowed the control of composition by simply adjusting the mixing ratio between the master batch

Table II. Mechanical Properties of PLA and PLA-CNW Single Fiber

Material	Young's modulus (MPa)	Tensile stress (MPa)	Elongation at break (%)	Shrinkage (%)
PLA	2500 ± 300	56 ± 7	62 ± 14	37
PLA-CNW$_1$	2500 ± 100	52 ± 7	13 ± 9	34
PLA-CNW$_3$	2700 ± 200	49 ± 3	10 ± 8	32

and the bulk PLA. The pellets on PLA and PLA with nanoadditives were prepared using the same processing parameters (see Figure 1). The third step was melt spinning of the pellets in a filament extruder to produce the nanocomposite fibers.

The melt spinning process was successful and PLA fibers were obtained from the compounds with and without nanowhiskers, in the temperature range of 190–210°C (see Table II and Figure 1). The spinning process proceeded smoothly with uptake velocity varying between 2 and 15 m/min, and at maximum winding speed of about 100 m/min. The fiber drawability was, however, found to be highly sensitive to the addition of CNWs and the draw ratio was limited to 2, due to fiber breakage. For PLA-based nanocomposite fibers with nanoclay a maximum draw ratio up to 3.5 has been reported,[15] whereas nanotube-based ones had draw ratios as high as 36.5.[16] The study on PLA-multiwalled nanotube fibers showed that the drawability of the fibers decreased with increasing concentration of nanoadditive, especially above 5 wt %.[16] In the current study the effect of concentration was not clear, as the nanoadditive content was relatively low and drawability was 2, at 1 and 3 wt % of CNWs.

Fiber Structure and Sizes

SEM was used to observe the surface of the fibers and the micrographs presented in Figure 2 show that both pure PLA and nanocomposite fibers have uniform diameters. Diameter measurements revealed that PLA fibers had an average diameter of 91 μm. However, after the addition of nanowhiskers the average diameter tended to increase to 92.5–94.6 μm [Figure 2(b)]. This trend may be explained by the fact that the viscosity of fibers increases when CNWs are added, resulting in less stretching of fibers and, consequently, a slightly larger diameter. However, this increase was not statistically significant and it was concluded that the fiber diameters were unaffected by the addition of nanowhiskers.

SEM also reveals that the surface roughness increased with increasing content of cellulose whiskers in PLA. This may be attributed to the aggregation of CNWs in the PLA matrix, which leads to formation of clusters on the surface of the fibers. This indicates that the CNWs are not uniformly dispersed in the PLA matrix. This is mainly due to the fact that CNWs have polar surfaces and require the presence of surfactants / compatibilisers for uniform dispersion in a nonpolar matrix like PLA. It may be noted that the fiber diameters obtained by melt spinning are much greater than those obtained by electrospinning, i.e., around 300 nm.[23] Furthermore, the surface roughness or CNW protrusion from the surface was not found for electrospun fibers, possibly indicating a better dispersion of CNWs in PLA. The processing method and use of solvent in electrospinning may be the reason for this.

The detailed morphology, studied using atomic force microscopy (AFM) with an aim to understand the dispersion of

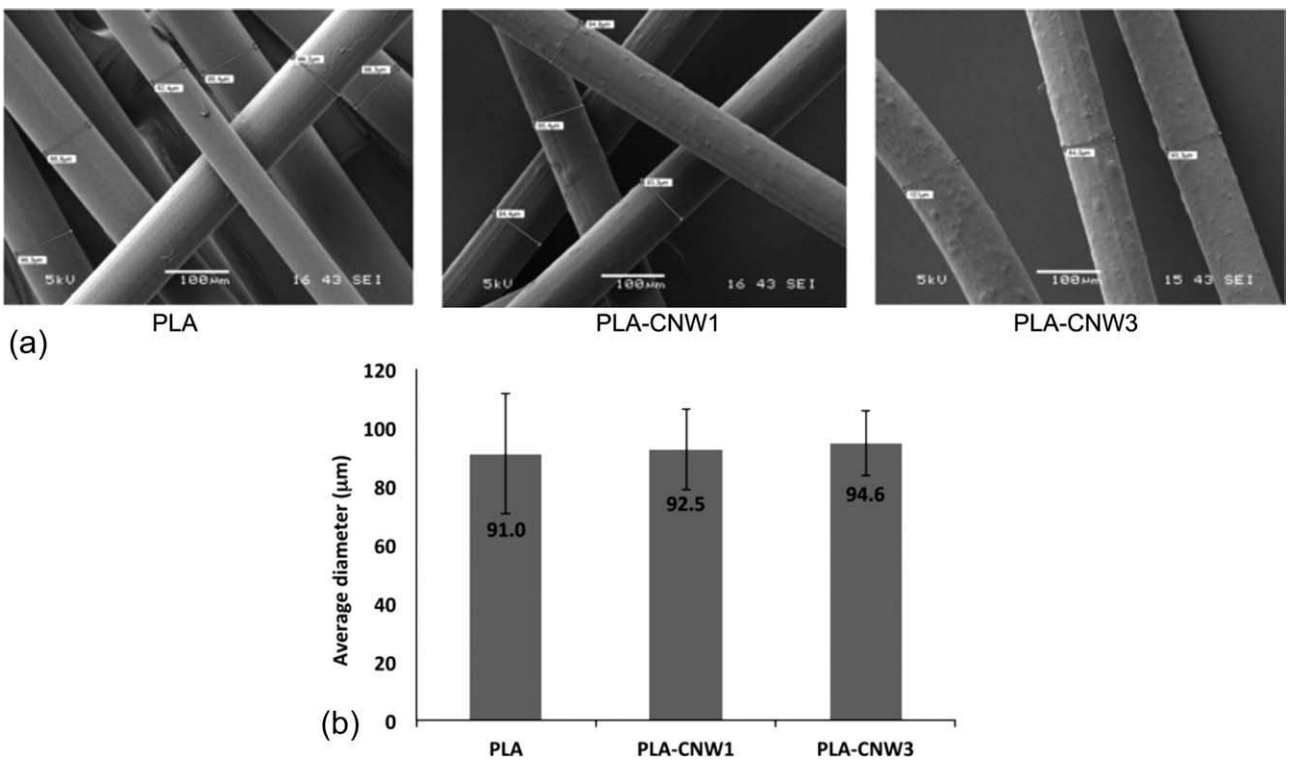

Figure 2. SEM of PLA based fibers and the average diameters measured based on SEM images.

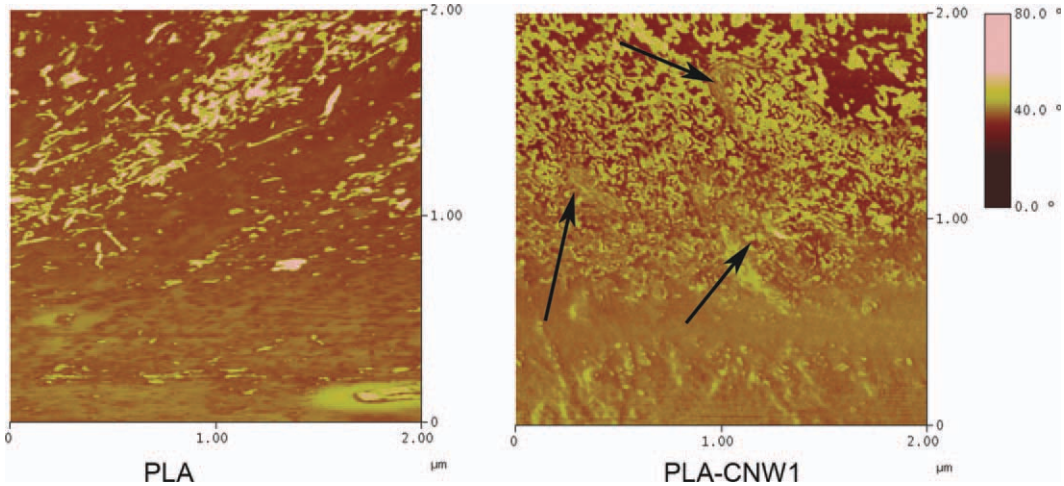

Figure 3. AFM image of PLA (a) and PLA–CNW_1 (b) fibers. The aggregates are marked with arrows. [Color figure can be viewed in the online issue, which is available at wileyonlinelibrary.com.]

CNWs in the PLA, is shown in Figure 3. The study of dispersion of CNWs in the PLA is challenging due to limitations with sample preparation and surface imaging issues related to the curvature of the fibers. The surface of PLA exhibits a homogenous phase with some striations that might have formed during the drawing of the fibers [Figure 3(a)]. PLA–CNW_1 [Figure 3(b)] shows regions with aggregates (marked with arrows) in the range of 1 micron and less. The nano-structured morphology indicates that the swelling and roughness found on the fiber surface in the SEM study may be due to cellulose nanowhisker aggregates. It was also noted that the AFM imaging did not give any information regarding the orientation of nanowhiskers in PLA matrix.

Mechanical Properties

The data obtained from the tensile tests are summarized in Table II, and the representative stress–strain curves are shown in Figure 4. It can be observed that the Young's modulus and the tensile strength of the PLA–CNW fibers did not change significantly compared to the PLA fibers. The average value of Young's modulus increased from 2500 to 2700 MPa for fibers containing 3% CNW. The tensile strength of the nanocomposite fibers, on the other hand, showed a slight decrease compared to the PLA fibers. No reports with nanocellulose as additive in melt-spun fibers, are available to date to compare the performance of the fibers in this study. In several studies, a decrease in tensile strength and/or modulus was reported for melt-spun fibers containing layered nanosilicates or nanoclay.[7,9,11,12,14,15] On the other hand, in a few systems, carbon nanotubes have had positive impact on the tensile strength and modulus.[10,13]

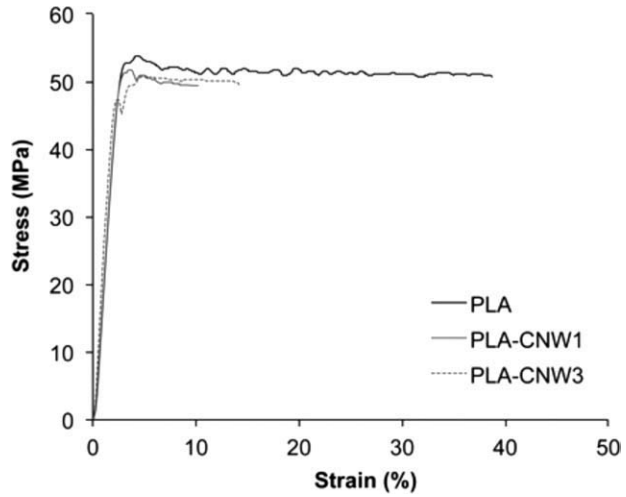

Figure 4. Stress–strain curves of PLA and PLA–CNW fibers.

In this study, it may be noted that the standard deviations for the Young's modulus and tensile strength data are too high to make any statistically significant conclusions. The elongation at break decreased significantly with the addition of CNWs. The strain at break decreased from 62 to 13% and to 10% with the addition of 1 and 3% of CNWs, respectively. The low tensile properties of PLA–CNW fibers compared to PLA fibers can be attributed to the imperfection introduced in the fibers due to aggregates of CNWs in the PLA as well as the poor interaction and compatibility between CNWs and the matrix resulting in poor stress transfer in nanocomposite fibers. Lee and Youn have shown that compatibilization had some positive impact on the tenacity of PP nanocomposite fibers reinforced with layered silicates. The authors observed an increase in tensile strength with addition of low concentrations of compatibiliser and also improvement in exfoliation of clay.[7] In this work, use of compatibilisers might also be a potential route to obtain improved interaction between the matrix and the nanoadditive, as well as to improve the dispersion.

Creep tests were performed to study the deformation in the fibers under constant temperature when subjected to stresses for a prolonged period of time. Figure 5 presents the variation in strain as a function of time. It can be observed that the creep values and permanent deformation are higher in PLA fibers and the addition of CNWs results in a decrease in creep. Similar results were observed by Alloin et al.[27] for ramie whisker reinforced poly(oxyethylene) nanocomposites prepared by solvent

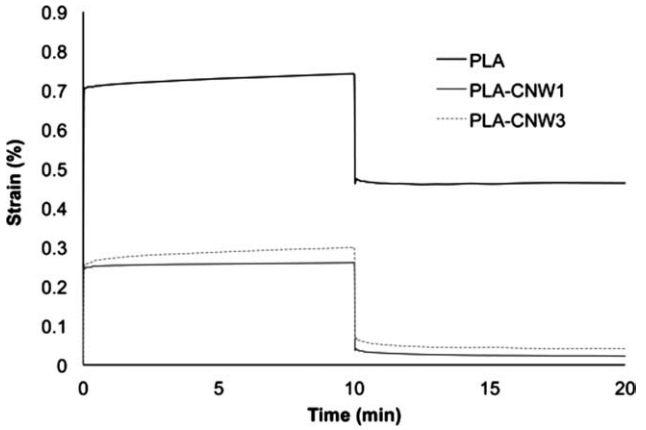

Figure 5. Creep behavior of PLA and PLA–CNW fibers at room temperature and at constant stress of 5 MPa.

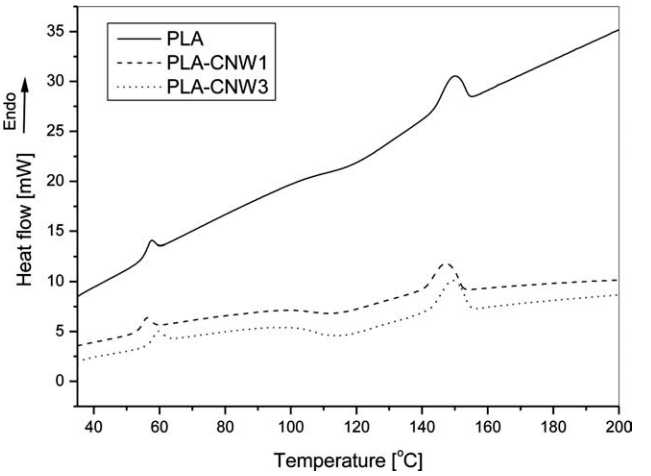

Figure 6. DSC thermograms of PLA-based fibers.

cast technique. This decreased creep in the presence of the nanoadditive suggests that the matrix mobility is restricted, at least at low stresses, compared to pure PLA. This restriction does not translate into increased mechanical properties at higher stresses, probably due to the nanoadditive aggregates acting as defects in the fiber.

Thermal Analysis

DSC measures the heat flow rate associated with a thermal event, thereby providing information about melting and phase transitions of the composite system. The thermograms and the representative values are presented in Figure 6 and Table III. All the studied materials exhibit glass transition, cold crystallization, and melt transition. The glass transition temperature of PLA was observed at 57°C, and only a marginal increase was found for the fibers containing 3% nanowhiskers. With regard to the melting temperature of the different samples, the addition of the CNWs in the PLA matrix causes only a marginal effect (±2°C), and no essential correlation of the results with the nanowhiskers content can be established. A comparison of crystallinity X_c of neat PLA, calculated according to eq. (1) for the PLA component in the nanocomposite fibers, yielded slightly higher values for the fibers containing nanowhiskers than those for pure PLA fibers. This observation can be explained by the fact that the surfaces of the CNWs act as nucleation sites for the crystallization and partial crystalline growth in PLA.[26,28] It may be assumed that the nucleating effect of the nanofiber surfaces contributes significantly to the occurrence of transcrystalline layers around the whiskers, resulting in an increase in the percentage of crystallinity. In a recent study, Pei et al. (2010) observed a marked improvement in crystallinity of functionalised cellulose whisker PLA compared to untreated composites. This was attributed to the nanostructured network with a highly dispersed nanocrystal phase and the associated larger specific surface area for crystallite nucleation.[29] In this study, a significant change in cold crystallization temperature was not observed; however, the nanocomposite fibers showed a broader cold crystallization temperature range than those of the pure PLA fibers. The thermal behavior of PLA also exhibits a cold crystallization process at 115°C, which is higher than that observed in electrospun PLA–CNW fibers (< 70°C).[23] Earlier reports have indicated that cellulosic additives can play a dual role in affecting the cold crystallization process of PLA.[26,28] Depending on the content and thermodynamic conditions, additives can act as heterogenous nucleating agents or physical hindrance to facilitate or retard the cold crystallization process.[27] On comparing the PLA-whisker fibers produced by electrospinning with those produced by melt spinning, it can be seen that at similar CNW contents (i.e., around 3 wt %) the effect of CNW addition on T_g, T_m, T_{cc}, and X_c is only marginal.[23] However, the percentage crystallinity obtained in the current study 16–19%) is slightly higher than that reported for electrospun fibers (8–11%).

The thermal stability and degradation profiles based on TGA are presented in Figure 7. The derivative thermogram (DTG)

Table III. DSC and TGA Results of PLA and PLA-CNW Fibers

	DSC					TGA			
Sample	Tm [°C]	ΔHm [J/g]	Tg [°C]	Tcc [°C]	Xc [%]	Tmax. [oC]	T10 [oC]	T80 [oC]	Char at 600°C [%]
PLA	149.0	14.64	57.0	115	15.7	370	328	371	0.2
PLA-CNW$_1$	147.0	14.80	56.1	111	15.9	380	348	396	1.1
PLA-CNW$_3$	149.7	17.90	59.7	113	19.2	393	348	399	2.8

T_m, melt temperature; ΔH_m, enthalpy of melting; T_g, glass transition temperature; T_{cc}, cold crystallization temperature; X_c, percentage crystallinity; T_{max}, Temperature of maximum degradation; T10, temperature for 10% degradation; T80, temperature for 80% degradation.

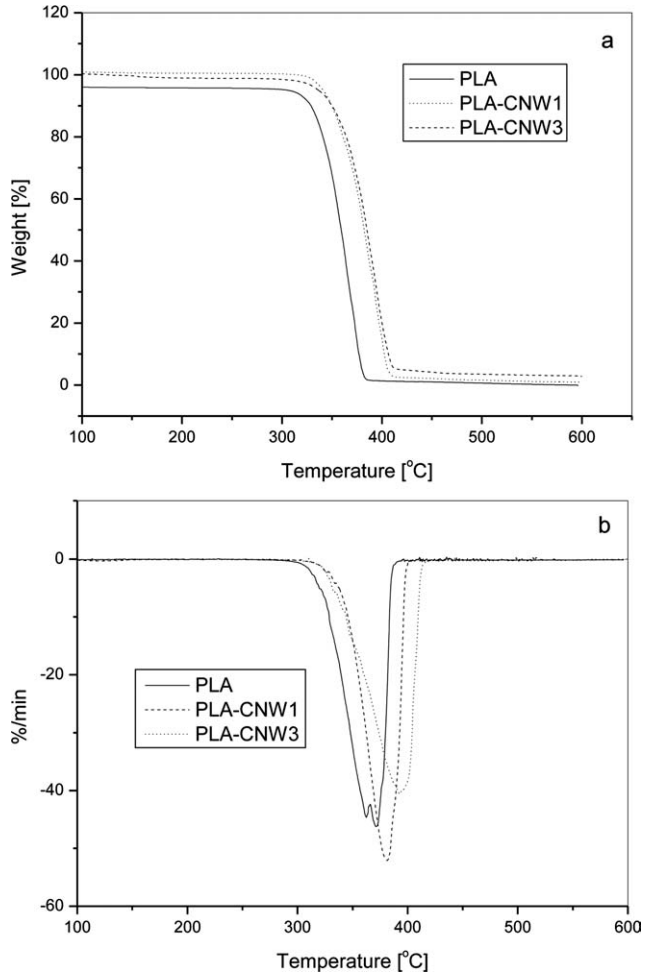

Figure 7. (a) TG and (b) DTG thermograms of PLA-based fibers.

tracing of PLA exhibits a single weight loss step with the maximum decomposition temperature at 370°C. The thermal decomposition process of the fibers with nanowhiskers also presented a single-step weight loss profile and was found to be stable in the temperature range of 30–275°C. In weight loss terms, the decomposition temperature at 10% weight loss occurred at 328°C for PLA (Table III), 348°C for fibers containing 1 and 3% cellulose whiskers [Figure 7(a)]. The major observations are that the peak degradation temperature of PLA fibers was found to be around 370°C, and the presence of 3% cellulosic whiskers increases the temperature to 393°C, resulting in a 6% increase in thermal stability. This can be attributed to the restriction of PLA polymer chain mobility in the vicinity of nanoadditive resulting in a delayed onset of degradation as well as diffusion of degradation products. Researchers have reported a similar increment in PLA composites with acetylated microfibrillated cellulose (MFC)[30] where the initial degradation temperature exhibited a 3% increase at 17% MFC loading. In another recent study, the authors observed a 14% increase in maximum degradation temperature upon the incorporation of 6% bacterial cellulose nanofibers in PLA matrix.[31] This was attributed to the good compatibility between PLA and bacterial cellulose nanofibers.

The shrinkage tests were performed at 80°C to understand the effect of temperature on the fiber structure. The shrinkage data are given in Table II. Relatively lower shrinkage was exhibited by the PLA–CNW_1 and PLA–CNW_3 compared to PLA fibers. This again indicates a decrease in molecular mobility of the polymer chains in the vicinity of the nanowhiskers. This makes the fibers containing nanowhiskers relatively less sensitive to heat and requires higher temperature to induce shrinkage. This data also support the increased thermal stability of the nanocomposite fibers found from the TGA results. This phenomenon of lower shrinkage has been observed earlier with PET and PLA fibers containing additives like nanoclay.[12,15,17] It may be noted that the shrinkage observed in the current study is higher (around 32%) than the other reports (<10%) with nanoclay. CNWs have the ability to reduce thermal shrinkage, although to a lesser degree compared to nanoclays.

CONCLUSIONS

This study focuses on the processing of cellulose whisker reinforced PLA nanocomposite fibers following a three-step process of master batch preparation, melt compounding, and fiber extrusion to form continuous fibers. The fibers were found to be relatively uniform and had diameters in the range of 70–95 μm. The addition of CNWs resulted in surface roughness. A study of the morphology using AFM showed the presence of aggregates of CNWs in micrometre range. The tensile strength of the fibers did not improve with the addition of CNWs, probably owing to the presence of aggregates and the lack of bonding between CNWs and PLA. However, the E-modulus values showed marginal improvement. DSC studies revealed that the crystallinity of fibers increased due to nucleating effect of whiskers. TGA results revealed a significant improvement of thermal stability in fibers containing CNWs. Furthermore, the fibers containing the nanoadditive exhibited higher creep resistance and lower shrinkage than PLA fibers. Generally, the results indicate possible restriction of polymer chain mobility in the presence of nanoadditives, which leads to positive impact on thermal stability, creep resistance and shrinkage reduction, which is overridden by the aggregation at high stresses.

From this initial study, it was concluded that although the processing was feasible, the dispersion and orientation processes of nanowhiskers upon extrusion are complex and still need to be improved. The increased heat stability and retarded shrinkage of the fibers with the addition of CNWs as well as the decreased creep, is expected to be of considerable interest in terms of bio-based industrial textiles and composite manufacture via textile routes. Future work will focus on improving the dispersion and mechanical properties of nanocomposite fibers by using compatibilisers and aligning the cellulose whiskers in the fibers.

ACKNOWLEDGMENTS

The authors gratefully acknowledge the financial support for this work from VINNOVA (Nanofiber), SIDA and the National Research Foundation (NRF), under project No. 348-2008-6009.

REFERENCES

1. Lee, S. M. *Handbook of Composite Reinforcements, Technology Engineering;* John Wiley & Sons, **1992**.
2. Solarski, S.; Ferriera, M.; Devaux, E. J. *Textil. Instit.* **2007,** *98*, 227.
3. Burkinshaw S. M.; Chemical Principles of Fiber Dyeing; Blackie Academic & Professional: London, **1995**, p 1.
4. Fourne, F. Synthetic Fibers, Machines and Equipments, Manufacture, Properties; Hanser Publishers: Munich, **1998.**
5. Choi, J.-H.; Kim, M.-H, Park, J.-S, Jeon, J.-M, Kim, D.-O, Towns, A. D. *Fibers Polym.* **2007,** *8*, 37.
6. Salem, D. R. Structure Formation in Polymeric Fibers; Hanser: Munich, **2001.**
7. Lee, S. H.; J Youn, J. *Appl. Polym. Sci.* **2008,** *109*, 1221.
8. Bourbigot, S.; Devaux, E.; Flambard X.; Polym. *Deg. Stab.* **2002,** *75*, 397.
9. Yoon, K.; Polk, M. B.; Min, B. G.; Schiraldi, D. A. *Polym. Int.* **2004,** *53*, 2072.
10. Rangari, V. K.; Yousuf, M.; Jeelani, S.; Pulikkathara, M. X.; Khabashekhu, V. N. *Nanotechnology* **2008,** *19*, 1.
11. Mazinan, S.; Ajji, A.; Dubios, C. *Polym. Eng. Sci.* **2010,** *50*, 1956.
12. Xaio, W.; Yu, H.; Han, K.; Yu, M. J. *Appl. Polym. Sci.* **2005,** *96*, 2247.
13. Anand, K. A.; Jose, T. S.; Agarwal, U. S.; Sreekumar, T. V.; Banwari, B.; Joseph, R. *Int. J. Polym. Mater.* **2010,** *59*, 438.
14. Mikalojczyk, T.; Rabeij, S.; Oejnik, M.; Urbanak-Domagala, W. J. *Appl. Polym. Sci.* **2007,** *104*, 339.
15. Solarski, S.; Ferreira, M.; Devaux, E.; Fontaine, G.; Bachelet, P.; Bourbigot, S.; Delobel, R.; Coszach, P.; Murariu, M.; Ferreira, A. D. S.; Alexandre, M.; Degee, P.; Dubois, P. *J. Appl. Polym. Sci.* **2008,** *109*, 841.
16. Potschke, P.; Andres, T.; Villmow, T.; Pegel, S.; Brunig, H.; Kobashi, K. *Comp. Sci. Technol.* **2010,** *70*, 343.
17. Solarski, S.; Mahjoubi, F.; Ferriera, M.; Deveaux, E.; Bachelet, P.; Bourbigot, S.; Delobel, R.; Coszach, P.; Maurariu, M.; Da Silva Ferriera, A.; Alexandre, M.; Degee, P.; Dubois, P. J. *Mater. Sci.* **2007,** *42*, 5105.
18. Murariu, M.; Doumbia, A.; Bonnaud, L.; Dechief, A. L.; Paint, Y.; Ferreira, M.; Campagne, C.; Devaux, E.; Dubois, P. *Biomacromolecules* **2011,** *12*, 1762.
19. Samir, M. A. S.; Alloin, F.; Dufresne, A. *Biomacromolecules* **2005,** *6*, 612.
20. Kvien, I.; Tanem, B. S.; Oksman, K. *Biomacromolecules* **2005,** *6*, 3160.
21. Oksman, K.; Mathew, A. P.; Bondeson, D.; Kvien, I. *Comp. Sci. Technol.* **2006,** *66*, 2776.
22. Mathew, A. P.; Chakraborty, .A.; Oksman, K.; Sain, M. **2006,** ACS Symposium Series 938, In Cellulose Nanocomposites Processing, Characterization and Properties; Oksman K. and Sain M., Eds.; Oxford University Press: Oxford, **2006,** p 656.
23. Liu, D.; Yuan, X.; Bhattacharya, D. J. *Mater. Sci.,* **2012,** *47*, 3159.
24. Bondesson, D.; Mathew, A. P.; Oksman, K.; *Cellulose* **2006,** *13*, 171.
25. Liu, X.; Dever, M.; Fair, N.; Benson, R. S.; *J. Environ. Polym Degrad.* **1997,** *5*, 225.
26. Mathew, A. P.; Oksman, K.; Sain, M.; *J. Appl. Polym. Sci.* **2006,** *101*, 300.
27. Alloin, F.; D'Aprera, A.; Dufresne, A.; Kissi, N. El.; Bossard, F. *Cellulose* **2011,** *18*, 957.
28. Wu, D.; Wu, L.; Xu, B.; Zhang, Y.; Zhang, M. J. *Polym. Sci.: Part B: Polym. Phys.* **2007,** *45*, 1100.
29. Pei, A.; Zhou, Q.; Berglund, L. A. *Comp. Sci. Technol.* **2010,** *70*, 815.
30. Tingaut, P.; Zimmermann, T.; Lopez-Suevos, F. *Biomacromolecules* **2009,** *11*, 454.
31. Tome, L. C.; Pinto, R. J. B.; Trovatti, E.; Freire, C. S. R.; Silvestre, A. J. D.; Neto, C. P.; Gandini, A. *Green Chem.* **2011,** *13*, 419.